**Syddansk Universitet**

# MicroRNA-4739 regulates osteogenic and adipocytic differentiation of immortalized human bone marrow stromal cells via targeting LRP3

Elsafadi, Mona ; Manikandan, Muthurangan ; Alajez, Nehad M; Hamam, Rimi; Dawud, Raed Abu; Aldahmash, Abdullah M.; Iqbal, Zafar ; Alfayez, Musaad ; Kassem, Moustapha; Mahmood, Amer

# MicroRNA-4739 regulates osteogenic and adipocytic differentiation of immortalized human bone marrow stromal cells via targeting LRP3

CrossMark

Mona Elsafadi [a,c], Muthurangan Manikandan [a], Nehad M Alajez [a], Rimi Hamam [a], Raed Abu Dawud [b], Abdullah Aldahmash [a,d], Zafar Iqbal [e], Musaad Alfayez [a], Moustapha Kassem [a,c], Amer Mahmood [a,*]

[a] *Stem Cell Unit, Department of Anatomy, College of Medicine, King Saud University, Riyadh 11461, Saudi Arabia*
[b] *Department of Comparative Medicine, King Faisal Specialist Hospital and Research Centre, Riyadh 12713, Saudi Arabia*
[c] *KMEB, Department of Endocrinology, University Hospital of Odense, University of Southern Denmark, Winslowsparken 25.1, DK-5000 Odense C, Denmark*
[d] *Prince Naif Health Research Center, King Saud University, Riyadh 11461, Saudi Arabia*
[e] *Department of Basic Sciences, College of applied medical sciences, King Saud Bin Abdulaziz University for Health Sciences (KSAU-HS), National Guard Health Affairs, Al Ahsa, Saudi Arabia*

## ARTICLE INFO

## ABSTRACT

Understanding the regulatory networks underlying lineage differentiation and fate determination of human bone marrow stromal cells (hBMSC) is a prerequisite for their therapeutic use. The goal of the current study was to unravel the novel role of the low-density lipoprotein receptor-related protein 3 (LRP3) in regulating the osteogenic and adipogenic differentiation of immortalized hBMSCs. Gene expression profiling revealed significantly higher LRP3 levels in the highly osteogenic hBMSC clone imCL1 than in the less osteogenic clone imCL2, as well as a significant upregulation of LRP3 during the osteogenic induction of the imCL1 clone. Data from functional and gene expression assays demonstrated the role of LRP3 as a molecular switch promoting hBMSC lineage differentiation into osteoblasts and inhibiting differentiation into adipocytes. Interestingly, microRNA (miRNA) expression profiling identified miR-4739 as the most under-represented miRNA ($-36.11$ fold) in imCL1 compared to imCL2. The TargetScan prediction algorithm, combined with functional and biochemical assays, identified *LRP3* mRNA as a novel target of miR-4739, with a single potential binding site for miR-4739 located in the *LRP3* 3′ UTR. Regulation of LRP3 expression by miR-4739 was subsequently confirmed by qRT-PCR, western blotting, and luciferase assays. Over-expression of miR-4739 mimicked the effects of LRP3 knockdown on promoting adipogenic and suppressing osteogenic differentiation of hBMSCs. Hence, we report for the first time a novel biological role for the LRP3/hsa-miR-4739 axis in balancing osteogenic and adipocytic differentiation of hBMSCs. Our data support the potential utilization of miRNA-based therapies in regenerative medicine.

## 1. Introduction

Throughout life, a homeostatic mechanism within the marrow cavity regulates fat and bone tissue formation. Both tissues originate from the same bone marrow progenitor cells; these are known as skeletal stem cells (SSCs), bone marrow-derived multipotent stromal cells, or mesenchymal stem cells (Bianco and Robey, 2004; Caplan, 1991; Friedenstein, 1976, 1968; Friedenstein et al., 1966; Owen and Friedenstein, 1988). SSCs are multipotent stromal cells that can differentiate into adipocytes, osteoblasts, or chondrocytes in response to various microenvironmental stimuli, including growth factors, cytokines,

and epigenetic regulators (Beresford et al., 1992; Gimble and Nuttall, 2004; Gimble et al., 1996). An imbalance between osteogenic and adipogenic lineage commitment and differentiation has been implicated as a cause of age-related impairment of bone formation. Thus, some therapeutic interventions have been proposed that aim to enhance bone mass by targeting SSCs and improving their functions (Yokota et al., 2002, 2003).

The low-density lipoprotein receptor-related protein (LRP) family is an evolutionarily conserved group of cell-surface receptors that regulate diverse biological functions in different organs, tissues, and cell types, in mammals and species of other taxa (Strickland et al., 1994; Croy et al., 2003). In addition to the function of LRPs as endocytic receptors that mediate the uptake of lipoproteins, several studies have demonstrated the involvement of these receptors in many cellular processes, including signal transduction, synaptic plasticity regulation, neuronal migration, cholesterol control, and vitamin homeostasis (Goretzki and Mueller, 1998; Trommsdorff et al., 1999; Gotthardt et al., 2000; Garcia et al.,

* Corresponding author at: P.O. Box 2925, 28, Riyadh 11461, Saudi Arabia.
  *E-mail addresses:* melsafadi@ksu.edu.sa, melsafadi@health.sdu.dk (M. Elsafadi),
nalajez@ksu.edu.sa (N.M. Alajez), dahmash@ksu.edu.sa (A. Aldahmash),
alfayez@ksu.edu.sa (M. Alfayez), mkassem@health.sdu.dk (M. Kassem),
ammahmood@ksu.edu.sa (A. Mahmood).

2001; Li et al., 2001a; Nykjaer and Willnow, 2002). LRP3 is an LRP family member expressed in a wide range of human tissues, with the highest expression observed in skeletal muscles and ovaries (Ishii et al., 1998). It has been reported that LRP3 modulates the cellular uptake of β-VLDL (Very Low Density Lipoprotein) (Ishii et al., 1998; Jeong et al., 2010). In contrast to LRP5 that has been demonstrated to participate in the canonical WNT pathway, bone formation, as well as in skeletal homeostasis and diseases (Abdallah et al., 2015; Clément-Lacroix et al., 2005; Haÿ et al., 2009; Kato et al., 2002; Williams and Insogna, 2009), the biological function of LRP3 has not been elucidated yet.

MicroRNAs (miRNAs) are a class of small, non-coding single-stranded RNAs (18–24 nucleotides) that modulate protein expression by binding to one or more types of mRNAs, which results in either translation repression or mRNA degradation (Ambros, 2004; Bartel, 2004; Pillai, 2005; Tétreault and De Guire, 2013). It has been reported that > 17.000 mature miRNA sequences are currently present in over 140 species, including plants, algae, viruses, and animals (Kozomara and Griffiths-Jones, 2011). These small molecules participate in the regulation of a variety of biological processes such as organ development, as well as cell proliferation, differentiation, motility, and apoptosis (Huang et al., 2010; Jia et al., 2014; Tétreault and De Guire, 2013). Since 2001, several studies have demonstrated an important role for a number of miRNAs in bone biology, as they were found to regulate osteoblastic and chondrogenic differentiation, as well as bone formation (i.e., ossification) (Dong et al., 2012; Laine et al., 2012a; Papaioannou et al., 2014; Pi et al., 2015; Eskildsen et al., 2011). Similarly, adipogenic differentiation has also been reported to be regulated by several miRNAs. This suggests a possible use of targeting miRNAs as therapeutic agents for enhancing bone formation by regulating the balance between the osteogenic and adipogenic differentiation processes (Skårn et al., 2012; Laine et al., 2012b; Hamam et al., 2014).

We recently described two immortalized human bone marrow stromal cell (hBMSCs) clones, imCL1 and imCL2, that were established through the over-expression of human telomerase reverse transcriptase (hTERT) in bone marrow-derived hBMSCs, with imCL1 exhibiting enhanced bone and fat formation compared to imCL2 (Elsafadi et al., 2016) In the current study, we established a novel regulatory network consisting of hsa-miR-4739 and LRP3 that balances the osteoblastic and adipocytic differentiation of hBMSCs.

## 2. Materials & methods

### 2.1. Cell culture

We employed a hBMSC-TERT cell line created from primary normal human bone marrow BMSCs by over-expressing the human telomerase reverse transcriptase gene (*hTERT*) (Abdallah et al., 2005; Al-Nbaheen et al., 2013). These cells have been extensively characterized and exhibit a cellular and molecular phenotype similar to that of primary hBMSCs (Al-Nbaheen et al., 2013). In the experiments described in this study, we employed two sub-clones derived from these hBMSCs, called imCL1 and imCL2, that exhibit enhanced or reduced osteogenic, adipogenic, and chondrogenic differentiation potential, respectively (Elsafadi et al., 2016). Human imCL1 and imCL2 cells were both cultured in Dulbecco's modified Eagle's medium (DMEM) supplemented with 4500 mg/L D-glucose, 4 mM L-glutamine, 110 mg/L sodium pyruvate, 10% fetal bovine serum (FBS), 1× penicillin-streptomycin (Pen-Strep), and non-essential amino acids. All culture reagents were purchased from Gibco (Thermo Fisher Scientific, Waltham, MA, USA).

### 2.2. siRNA-mediated transfection of hBMSCs

Cells in logarithmic growth phase were reverse-transfected with 25 nM of the Ambion Silencer Select Pre-designed LRP3-siRNA (Assay ID: s8284, Cat. No. 4390824; Thermo Fisher Scientific) or the Ambion Silencer Select Negative Control No. 2 siRNA (Cat. No. 4390846; Thermo

Fisher Scientific) using the Invitrogen Lipofectamine RNAiMAX Reagent (Thermo Fisher Scientific) plus serum-free Gibco Opti-MEM I medium (Thermo Fisher Scientific) as per the manufacturer's recommended protocol. On the third day post-transfection, cells were induced to osteogenic or adipogenic differentiation and then incubated for an additional week.

### 2.3. Alamar Blue cell viability/proliferation assay

Cell viability was evaluated using the Alamar Blue assay according to the manufacturer's recommendations (Cat. No. BUF012B; AbD Serotec, Raleigh, NC, USA). In brief, 10 μL of Alamar Blue substrate was added to cultured cells in 96-well plates, followed by incubation in the dark at 37 °C for 1 h. Readings were subsequently taken using a Synergy II microplate reader (BioTek Instruments, Winooski, VT, USA) set at fluorescent mode (excitation wavelength, 530 nm; emission wavelength, 590 nm).

### 2.4. Western blotting

Whole cell lysates were prepared as previously described (Elsafadi et al., 2016). Total proteins were analyzed by blotting with anti-LRP3 (Cat. No. ab112581, rabbit anti-human LRP3 antibody, 83 kDa, dilution 1:250; Abcam, Cambridge, UK), and anti-β-actin (Cat. No. A3854, dilution 1:10,000; Sigma-Aldrich, St. Louis, MO, USA). Non-immune immunoglobulin of the same isotype was used as a negative control. Reactivity was detected with horseradish peroxidase-conjugated secondary antibodies (Santa-Cruz Biotechnology, Dallas, TX, USA) and Clarity Western ECL substrate (Bio—Rad, Hercules, CA, USA). Produced chemiluminescence was measured using a C-Digit Blot Scanner (LI-COR Biosciences, Lincoln, NE, USA).

### 2.5. In vitro osteoblast differentiation

Cells were grown in 6-well plates, standard DMEM, and at a density of $0.3 \times 10^6$ cells/mL. When cells reached 70–80% confluence, they were cultured in DMEM supplemented with an osteogenic induction supplements containing 10% FBS, 1% Pen-Strep, 50 μg/mL L-ascorbic acid (Wako Chemicals, Neuss, Germany), 10 mM β-glycerophosphate (Sigma-Aldrich), 10 nM calcitriol (1α,25-dihydroxyvitamin D3; Sigma), and 10 nM dexamethasone (Sigma-Aldrich). The medium was replaced three times per week.

### 2.6. In vitro adipocyte differentiation

Cells were grown in standard DMEM, 6-well plates at 20,000 cells/cm². At 90–100% confluence, cells were cultured in DMEM supplemented with an adipogenic induction mixture containing 10% FBS, 10% Horse Serum (Sigma-Aldrich), 1% Pen-Strep, 100 nM dexamethasone, 0.45 mM isobutyl methylxanthine (Sigma-Aldrich) (Hildebrand et al., 1994), 3 μg/mL insulin (Sigma-Aldrich), and 1 μM rosiglitazone (Serra and Chang, 2003). Medium was replaced 3 times per week.

### 2.7. Cytochemical staining

#### 2.7.1. Alizarin Red S staining of mineralized matrix

Cell layers were washed with PBS and then fixed with 4% paraformaldehyde (Sigma-Aldrich) for 15 min at room temperature. After removing the fixative, each cell layer was rinsed with distilled water and then stained with 2% Alizarin Red S (Alizarin Red S Staining Kit; Cat. No. 0223; Sciencell Research Laboratories, Carlsbad, CA, USA) for 20–30 min at room temperature. Excess dye was washed away with water. For quantification, the bound dye was first eluted by incubating each stained cell layer with 800 μL of acetic acid for 30 min at room temperature as previously described (Gregory et al., 2004), and then

measured using an Epoch spectrophotometer (BioTek Instruments) at 405 nm.

### 2.7.2. OsteoImage mineralization assay

The mineralized matrix was quantified using the OsteoImage Mineralization Assay Kit (Cat. No. PA-1503; Lonza, Allendale, NJ, USA). After removal of the culture medium, cells were washed once with PBS and then fixed with 70% cold ethanol for 20 min. The appropriate amount, as recommended by the manufacturer, of diluted staining reagent was added, and the plates were incubated in the dark for 30 min at room temperature. Afterwards, cells were washed, and the bound reagent was quantified using a fluorescent plate reader (excitation wavelength, 530 nm; emission wavelength, 590 nm).

### 2.7.3. Oil Red-O staining of lipid droplets

Mature adipocytes filled with cytoplasmic lipid droplets were visualized by staining with Oil Red-O. After washing with PBS, the cells were fixed in 4% formaldehyde for 10 min at room temperature, rinsed once with 3% isopropanol, and stained for 1 h at room temperature using filtered Oil Red-O staining solution (prepared by dissolving 0.5 g Oil Red-O powder in 60% isopropanol). Quantification of the formed mature adipocytes was performed by adding 100% isopropanol to each well to elute the bound Oil Red-O stain and then measuring color intensity using the BioTek Epoch spectrophotometer at 510 nm.

### 2.7.4. Nile Red fluorescence determination and quantification of mature adipocytes

The stock solution of Nile Red (1 mg/mL in DMSO) was prepared and stored protected from light at −20 °C. Cultured undifferentiated and differentiated cells were fixed with 4% paraformaldehyde for 15 min and then washed once with PBS. Afterwards, a 5 μg/mL dye solution in PBS was added directly to the cells. After 10 min of incubation at room temperature, the fluorescence signal was measured using a SpectraMax/M5 fluorescence spectrophotometer plate reader (Molecular Devices, Sunnyvale, CA, USA) set at bottom well-scan mode. Nine readings were measured per well (excitation wavelength, 485 nm; emission wavelength, 572 nm).

### 2.8. Quantitative real time PCR (qRT-PCR)

Total RNA was extracted using the Ambion PureLink RNA Mini Kit (Cat. No. 12183018A; Thermo Fisher Scientific) as recommended by the manufacturer, and quantified by a Nanodrop 2000 spectrophotometer (Thermo Fisher Scientific). Complementary DNA (cDNA) was synthesized from 1 μg RNA using the Applied Biosystems High Capacity cDNA Reverse Transcription Kit (Thermo Fisher Scientific) in a Multigene thermocycler (Labnet International, Edison, NJ, USA) according to the manufacturer's instructions. Relative mRNA levels were determined from cDNA by real-time PCR using the Applied Biosystems Real Time PCR Detection System (Thermo Fisher Scientific), with the
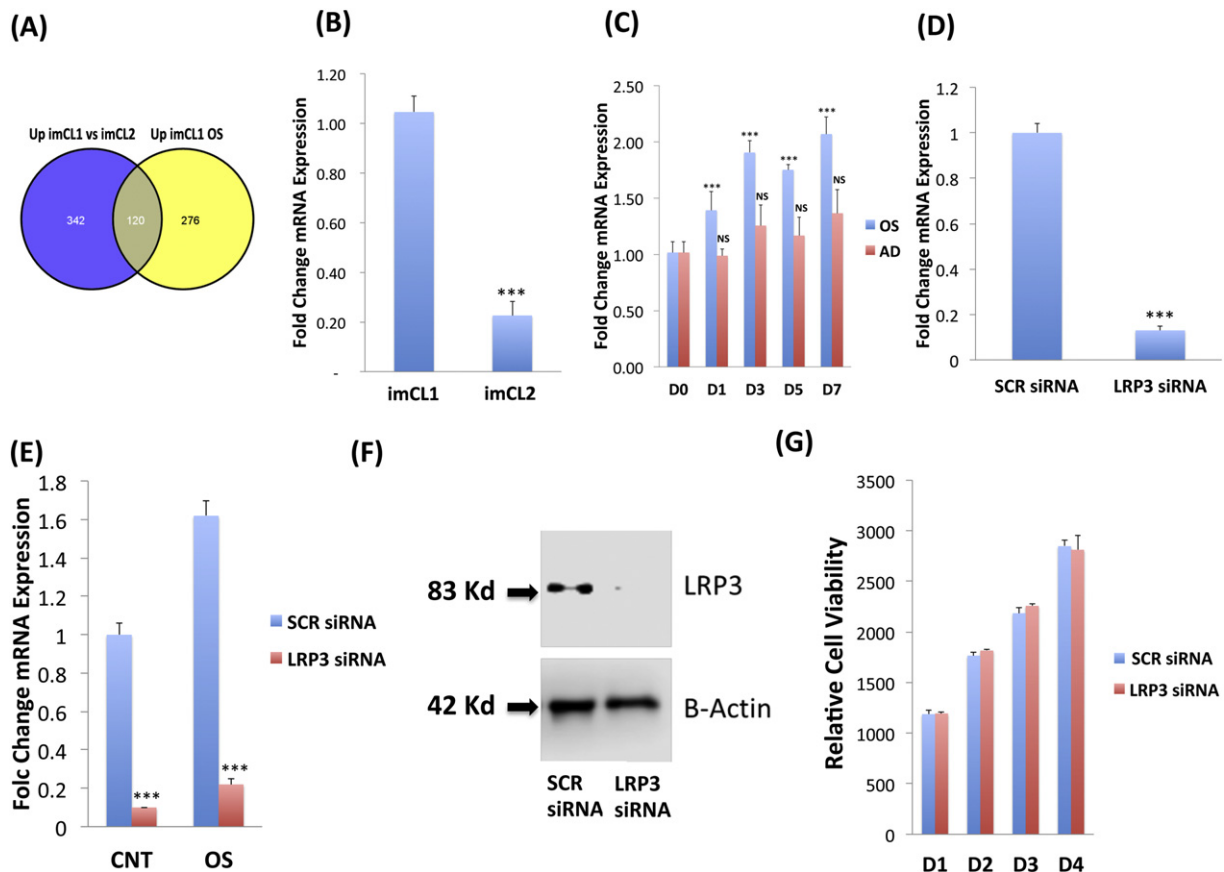


**Fig. 1.** Expression of LRP3 during in vitro differentiation of imCL1 and imCL2 cells. (A) Venn diagram depicting the overlap between the group of differentially over-represented genes in imCL1 and imCL2 cells, and the group of over-represented genes during the osteogenic differentiation (day 7) of imCL1 cells (B) Quantitative TaqMan Real-Time PCR for determining *LRP3* mRNA levels in imCL1 and imCL2 cells. (C) QRT-PCR quantification of *LRP3* transcript at different time points [D0 (non-induced), D1, D3, D5, and D7] during osteogenic and adipogenic differentiation of imCL1 cells. (D) QRT-PCR quantification of *LRP3* mRNA on day 3 post-transfection with LRP3-specific or scrambled control siRNA. Data are presented as fold change of mRNA levels in LRP3-siRNA-transfected cells compared to those of cells transfected with scrambled siRNA. (E) QRT-PCR quantification of *LRP3* mRNA in imCL1 cells transfected with LRP3-siRNA or scrambled-control siRNA, at baseline and on day 3 post osteogenic induction. *GAPDH* mRNA levels were used as a normalizer. Data are presented as mean ± SD, n = 3. Each experiment was performed at least two times; *P < 0.05; **P < 0.01, ***P < 0.005. (F) Representative western blots for LRP3 protein in scrambled-siRNA- or LRP3-siRNA-transfected cells. β-Actin was used as a loading control. (G) Alamar Blue determination of cell viability performed on scrambled-siRNA- or LRP3-siRNA-transfected cells at the indicated time points. No differences in cell viability between the two groups were observed.

Applied Biosystems Power SYBR Green PCR Kit (Thermo Fisher Scientific) or the Applied Biosystems TaqMan Universal Master Mix II without Uracil-N-Glycosylase (UNG) (Thermo Fisher Scientific), according to the manufacturer's instructions. Following normalization to the reference gene *GAPDH*, quantification of gene expression was carried out using a comparative CT method where ΔCT is the difference between the CT values of the target and the reference gene. Primers used in the current study are listed in Supplementary Tables 4 and 5.

### 2.9. DNA microarray global gene expression profiling

Total RNA was extracted with the Ambion PureLink RNA Mini Kit following the manufacturer's instructions. Afterwards, 150 ng of total RNA was labeled and then hybridized to the Agilent Human SurePrint G3 Human GE 8 × 60 k microarray chip (Agilent Technologies, Santa Clara, CA, USA). All microarray experiments were conducted at the Microarray Core Facility of the Stem Cell Unit, Anatomy Department, College of Medicine, King Saud University. Normalization and data analyses were performed using the GeneSpring GX software (Agilent Technologies). Pathway analysis was conducted using the Single Experiment Pathway analysis feature of GeneSpring 12.0 (Agilent Technologies). A fold change (FC) of two with P < 0.02 was chosen as cutoff.

### 2.10. miRNA expression profiling

MicroRNA expression profiling of imCL1 and imCL2 cells was conducted. First, total RNA was extracted with the Total RNA Purification Kit (Cat. No. 37500; Norgen, Thorold, ON, Canada), and 200 ng was used for RNA labeling and hybridization onto the Human SurePrint G3

8 × 60 k v16 miRNA microarray chip (Agilent Technologies) according to the manufacturer's protocol. Data were subsequently normalized and analyzed using GeneSpring GX. A FC of two with P < 0.01 was used as cutoff to determine the differentially expressed miRNAs between imCL1 and imCL2 (Elsafadi et al., 2016). Target prediction was conducted based on the TargetScan database, using the corresponding built-in feature of GeneSpring GX.

### 2.11. miRNA transfection

The reverse transfection approach was used as described before (Alajez et al., 2011) for the miRNA mimic Ambion Negative Control No. 1 (Cat. No. 4464058; Thermo Fisher Scientific) and the Ambion hsa-miR-4739 (Cat. No. 4464066; Thermo Fisher Scientific). Briefly, miRs were diluted in 50 μL of Gibco Opti-MEM (Cat. No. 11058-021; Thermo Fisher Scientific) to a final concentration of 60 nM, whereas 1.5 μL of Invitrogen Lipofectamine 2000 (Part No: 52758; Thermo Fisher Scientific) was diluted in 50 μL Opti-MEM. The diluted miR-mimics, siRNA, and Lipofectamine 2000 were mixed and incubated at ambient temperature for 20 min. The transfection mixture was then added to 24-well cell culture plates (100 μL per well), followed by the addition of 400 μL transfection medium (routine culture medium without antibiotics) containing 50,000 cells to each well. Every experiment included the appropriate controls, was performed in triplicate, and was repeated at least two times. Plates were incubated for the indicated time points, and proliferation or growth inhibition was assessed using the Alamar Blue assay, as described in 2.3.
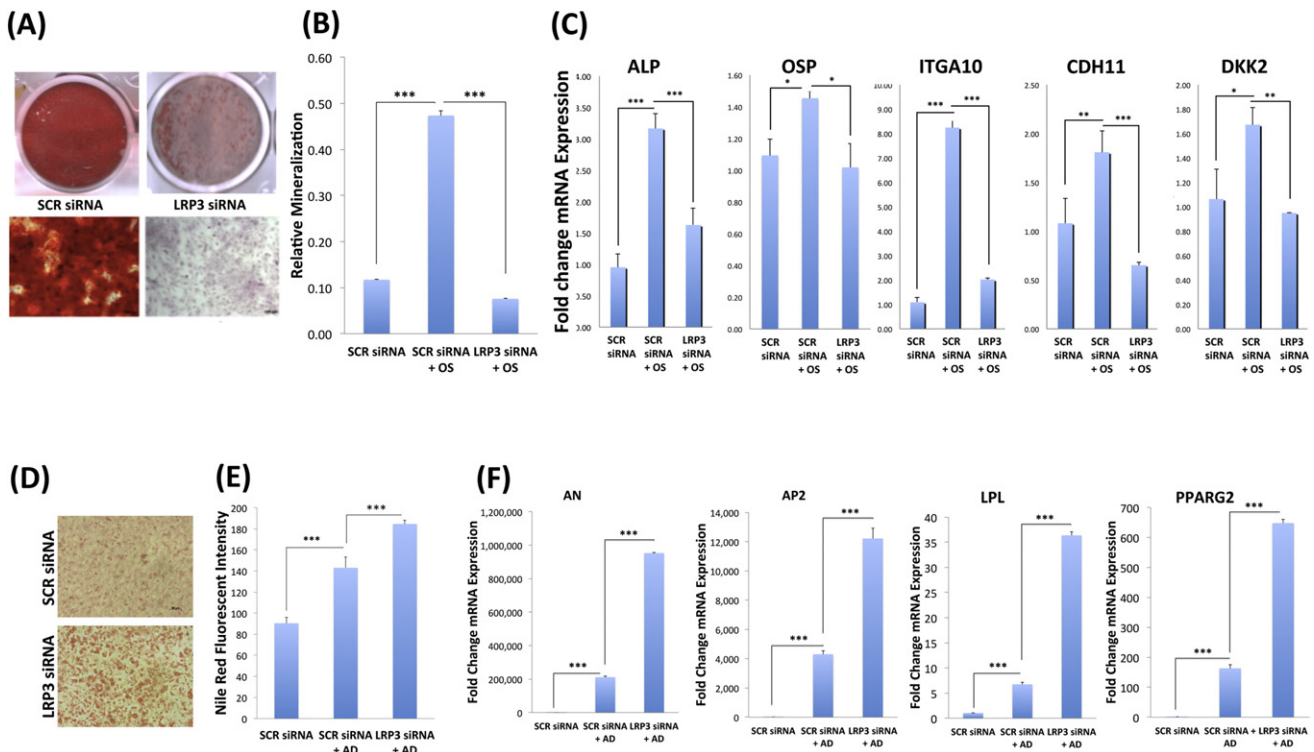


Fig. 2. LRP3 silencing inhibits osteogenesis and promotes adipogenesis in imCL1 cells. (A) imCL1 cells were differentiated into osteoblasts by treatment with an osteogenic mixture for 5 days. Mineralized calcium deposition was determined by Alizarin Red S staining. Scanned images of stained wells are displayed. Representative images were taken at 10× magnification. (B) Quantification of mineralized calcium deposition under different treatment conditions: non-induced scrambled-siRNA-transfected cells, osteogenic-induced scrambled-siRNA-transfected cells, and osteogenic-induced LRP3-siRNA-transfected cells. (C) QRT-PCR for osteogenic gene markers (*ALPL, OSP, ITGA10, CDh11,* and *DKK2*) under different treatment conditions: non-induced scrambled-siRNA transfected cells, osteogenic-induced scrambled-siRNA-transfected cells, and osteogenic-induced LRP3-siRNA-transfected cells. (D) imCL1 cells transfected with scrambled or LRP3 siRNA were induced with an adipogenic mixture for 5 days and stained using Oil Red-O for accumulated oil droplets. (E) Quantification of oil content using Nile Red staining after different treatments: non-induced scrambled-siRNA-transfected, adipogenic-induced scrambled-siRNA-transfected, and adipogenic-induced LRP3-siRNA-transfected cells. (F) Total RNA was extracted and qRT-PCR was performed for the adipogenic marker genes *ADIPOQ, AP2, LPL,* and *PPARG*. Results are representative of at least two independent experiments. Data are presented as mean ± SD, n = 3; *P < 0.05; **P < 0.01, ***P < 0.005.

## 2.12. Luciferase assay

To determine whether hsa-miR-4739 directly interacts with the 3′ untranslated region (3′-UTR) of the *LRP3* mRNA, HEK-293 cells were co-transfected with 30 nM of either miR-CNT (control) or miR-4739 mimics, and 50 ng/μL of either the miTarget negative control clone (Cat. No. CmiT000001-MT05; GeneCopoeia, Rockville, MD, USA) or the LRP3 miTarget miRNA 3′-UTR Clone (Cat. No. HmiT1010872-MT05; GeneCopoeia). Transfection experiments were conducted using Invitrogen Lipofectamine 2000. At 72 h post transfection, Gaussia luciferase (Gluc) activity was measured using the Secrete-Pair Luminescence Assay Kit (GeneCopoeia). Secreted alkaline phosphatase (SEAP) activity was used for normalization as we previously described (Vishnubalaji et al., 2016).

## 2.13. Statistical analysis

All results were presented as mean ± SD (standard deviation) of at least two independent experiments. Each experiment was performed in triplicate. Student's *t*-test was used for evaluating differences between groups. P < 0.05 was considered statistically significant.

## 3. Results

### 3.1. Expression of LRP3 during immortalized hBMSC differentiation

We recently established two **immortalized** hBMSC clones, namely imCL1 and imCL2, exhibiting remarkable differences in their osteogenic and adipocytic differentiation potentials. Specifically, imCL1 displays enhanced osteogenic and adipocytic differentiation compared to imCL2 (Elsafadi et al., 2016). Gene expression profiling identified 462 genes that were over-represented in the imCL1 compared to the imCL2 line (Supplementary Table 1). When CL1 cells were subjected to osteogenic differentiation, 396 genes were over-represented (Supplementary Table 1). Interestingly, 120 of these 396 genes also belonged to the group of 462 genes whose expression was higher in imCL1 compared to imCL2 cells (Fig. 1A, Supplementary Table 1). LRP3 was the most prominent among these 120 genes (FC = 6.6, P < 0.05, imCL1 vs. imCL2 cells, Fig. 1B). QRT-PCR analysis revealed a significant increase in LRP3 mRNA levels during in vitro osteogenic differentiation, while no significant changes were observed during adipocytic differentiation (Fig. 1C). In follow-up experiments, we carried out siRNA-mediated silencing of *LRP3* in the presence or absence of osteogenic induction medium. QRT-PCR confirmed a significant down-regulation of *LRP3* mRNA
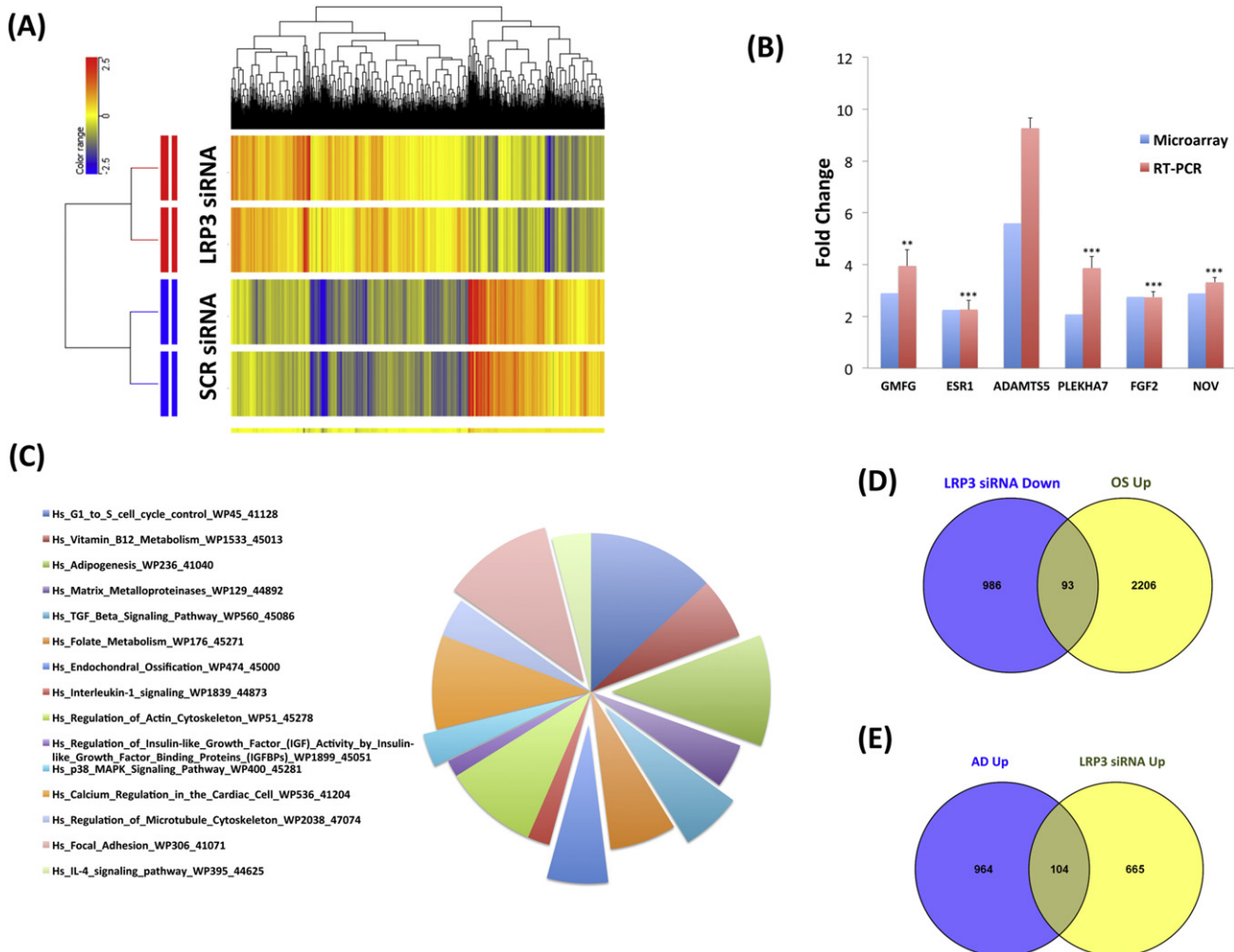


**Fig. 3.** Gene expression profiling of LRP3-depleted cells. (A) Hierarchical clustering of parental scrambled cells and LRP3-depleted cells based on the levels of differentially expressed mRNAs. Each row represents one replica, and each column represents a transcript. The expression level of each gene in a single sample is depicted according to the color scale. (B) QRT-PCR validation of the microarray data for selected genes; n = 3, *P < 005, ***P < 0001. Scrambled cells were used as a control. (C) Pie chart illustrating the distribution of the top pathway designations for the deregulated genes in LRP3-siRNA transfected cells. (D) Venn diagram illustrating the overlap between the differentially over-represented genes during the osteogenic differentiation of scrambled imCL1 cells and the under-represented genes after LRP3 knockdown. (E) Venn diagram illustrating the overlap between the differentially over-represented genes during the adipogenic differentiation of scrambled imCL1 cells and the over-represented genes after LRP3 knockdown.

expression (Fig. 1D–E), while western blot analysis confirmed the suppression of LRP3 expression at the protein level (Fig. 1F). LRP3-deficient in imCL1 did not exhibit changes in cell proliferation, as determined by the Alamar Blue viability and proliferation assay (Fig. 1G).

## 3.2. LRP3-deficient cells showed impaired osteoblastic and enhanced adipocytic differentiation

To investigate the potential role of LRP3 in regulating imCL1 differentiation, imCL1 cells were transfected with LRP3 siRNA and then exposed to osteogenic induction medium. LRP3-siRNA-transfected imCL1 cells exhibited impaired osteoblast differentiation. This was demonstrated by both a significant reduction in mineralized matrix formation, as visualized by Alizarin Red staining (Fig. 2A–B). Furthermore, there was decreased expression of osteoblastic markers *TNAP* (tissue non-specific alkaline phosphatase), *SPP1* (osteopontin), *ITGA10* (integrin alpha-10), *CDH11* (cadherin-11), and *DKK2* (dickkopf-related protein-2) (Fig. 2C). In contrast, LRP3-deficient imCL1 cells exhibited enhanced adipocytic differentiation, as shown by an increased number of lipid-filled mature adipocytes, quantified by Nile Red staining (Fig. 2D–E) and over-represented expression of a panel of adipocytic markers, namely *AN* (adiponectin), *aP2* (adipocyte Protein 2), *LPL*

(Lipoprotein Lipase), and *PPARG* (Peroxisome Proliferator Activated Receptor Gamma) (Fig. 2F).

## 3.3. Molecular signature of LRP3-deficient imCL1 cells

To determine the molecular mechanism mediating the functions of LRP3 in hBMSCs, we performed global gene expression profiling of imCL1 transfected with LRP3 siRNA or scrambled control siRNA. Hierarchical clustering revealed that control cells and LRP3-deficient cells clustered separately (Fig. 3A). We found that 1709 genes were over-represented and 1022 genes under-represented in LRP3-deficient cells compared to control cells (FC ≥ 2.0, P < 0.02). To confirm the microarray data, we performed qRT-PCR for selected genes of these two groups that are known to be involved in cell differentiation and the TGFβ pathway. Results showed a good concordance between microarray and qRT-PCR data (Fig. 3B). Bioinformatics analysis revealed that LRP3-deficient cells exhibited enrichment in genes belonging to several intracellular signaling pathways, including pathways related to the regulation of the actin cytoskeleton, focal adhesions, endochondral ossification, adipogenesis, the TGFβ signaling pathway, and the MAPK cascade (Fig. 3C). We subsequently identified the genes that might be associated with the impaired osteogenic and augmented adipocytic differentiation of LRP3-deficient imCL1 cells. Data revealed 93 genes shared by the
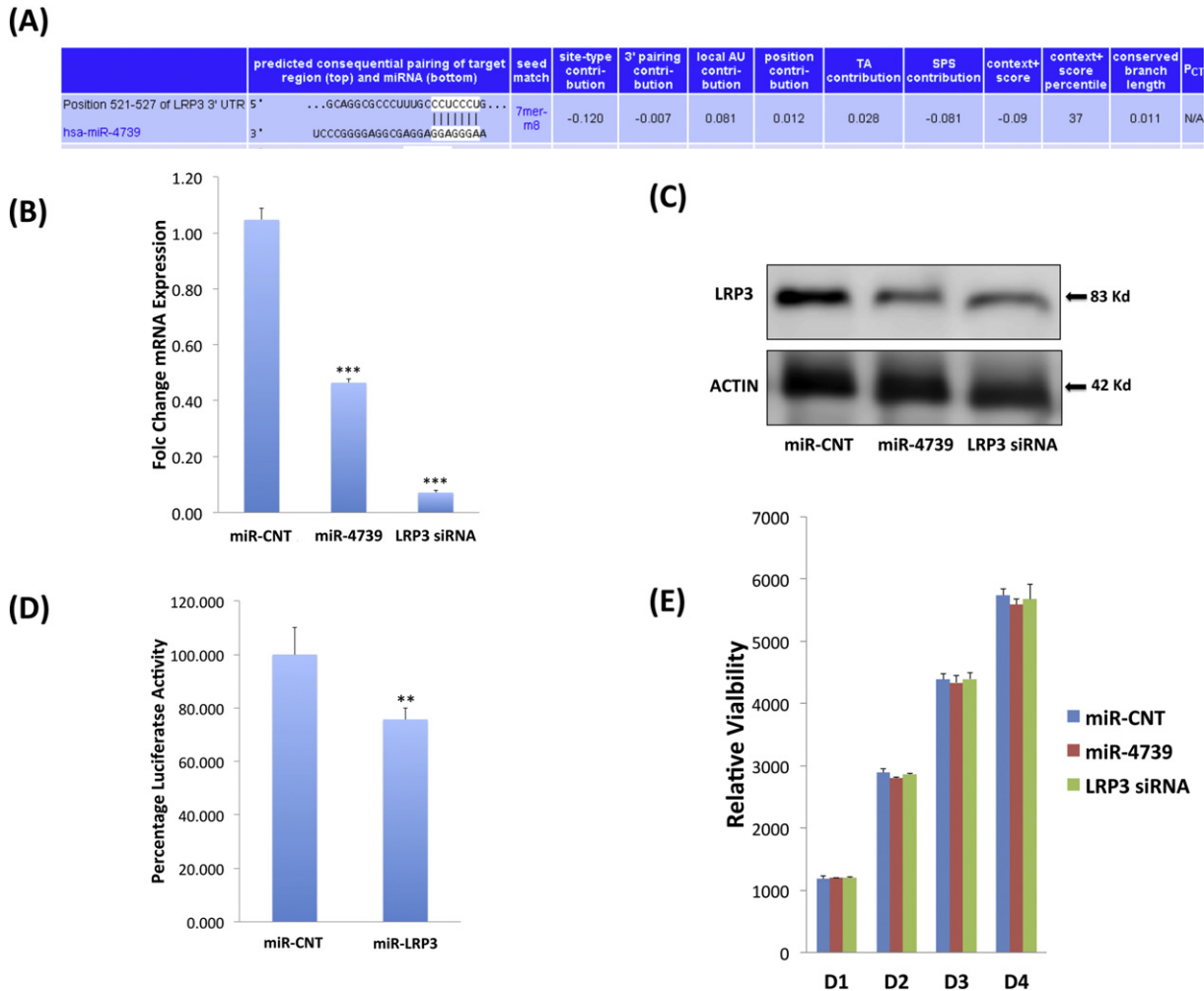


**Fig. 4.** Direct regulation of LRP3 by miR-4739. (A) Schematic presentation showing the alignment of the mature hsa-miR-4793 sequence and the putative binding site in the 3′-UTR region of the *LRP3* mRNA. The TargetScan database was used. The exact positions where the *LRP3* 3′-UTR and the miR-4739 seed region interact are indicated. (B—C) Over-expression of hsa-miR-4739 was associated with a significant decrease in *LRP3* mRNA (B) and protein (C); ***P < 0.005. LRP3-siRNA-transfected cells were used as a positive control. (D) *LRP3* 3′-UTR or a control vector were co-transfected with a miR control (30 nM) or miR-4739 (30 nM) mimics in HEK-293 cells. Gluc luciferase activity was measured 72 h following transfection, while luciferase activity from SEAP was used for data normalization. Data are presented as mean ± S.D., n = 6; **P < 0.005. (E) Alamar Blue quantification of cell viability in the first four days post-transfection of imCL1 cells with hsa-miR-4739, LRP3-siRNA, or pre-miR-control.

group of genes that were under-represented in LRP3-deficient cells and the group of genes that were over-represented during the osteoblastic differentiation of control hBMSCs (Fig. 3D, Supplementary Table 2). Among these 93 genes, *TWIST1*, *TBXAS1*, *CALCA*, *PDE4D*, *ASPN*, *TGIF1*, *PIM1*, *NFIA*, *C5AR1*, *CSGALNACT1*, and *HOXDA* have been previously shown to play a role during osteogenesis and bone development (Chen et al., 2015; Driller et al., 2007; Fromental-Ramain et al., 1996; Geneviève et al., 2008; Huebner et al., 2008; Kalbasi Anaraki et al., 2014; Kim et al., 2010a; Quarto et al., 2015; Sato et al., 2011; Ueda et al., 2016; Wakabayashi et al., 2002). On the other hand, 104 genes were over-represented in LPR3-deficient imCL1 cells as well as in control cells differentiated into adipocytes. Among those, *APOE*, *ANGPTL4*, *CES1*, *CBS*, *DUSP1*, *BMP6*, *ATF3*, *SAA1*, *BTG2*, *GDF15*, *CPE*, *LRP1B*, and *ADHFE1* have been previously reported to play a role during adipogenesis (Chiba et al., 2003; Ferguson et al., 2015; Jang and Jung, 2014; Jernås et al., 2009; Kim et al., 2007, 2016; Masson et al., 2009; Min et al., 2005; Sharma et al., 2014; Tsai et al., 2015; Wang et al., 2015b, 2010; Yanagitai et al., 2012) (Fig. 3E and Supplementary Table 3).

### 3.4. miR-4739 mediates its biological effects through targeting LRP3

We subsequently investigated the mechanism underlying LRP3 up-regulation in imCL1 cells. MicroRNA expression profiling revealed that hsa-miR-4739 is one of the most down-regulated miRNAs in imCL1 compared to imCL2 cells (FC = −36.11 fold; Table 1), suggesting a plausible role for this miRNA in regulating hBMSC differentiation. In silico predictions conducted with the TargetScan algorithm revealed a single potential binding site for hsa-miR-4739, located in the 3′-UTR of the *LRP3* mRNA (Fig. 4A). The role of hsa-miR-4739 in regulating LRP3 expression was confirmed by qRT-PCR and western blotting, which showed suppression of *LRP3* mRNA and protein expression, respectively, in hsa-miR-4739 transfected imCL1 cells (Fig. 4B–C). Cells

transfected with siRNA against *LRP3* were used as a positive control. To confirm that the *LRP3* mRNA is indeed a direct target for hsa-miR-4739, we performed a luciferase reporter assay. HEK-293 cells were co-transfected with an *LRP3* 3′-UTR reporter clone in which the *LRP3* 3′-UTR was cloned downstream of the *Gluc* gene. The vector also contained the *SEAP* gene as a transfection control. Results revealed a significant suppression (~30%) of luciferase activity produced by the *LRP3* 3′-UTR reporter clone in an hsa-miR-4739-dependent manner (Fig. 4D). No significant difference was observed in cell viability or proliferation between cells transfected with miR-control, hsa-miR-4739, or LRP3 siRNA during the four-day follow-up period (Fig. 4E).

### 3.5. 3.5. Identification of miR-4739 as bona fide regulator of hBMSCs differentiation

To examine the biological role of hsa-miR-4739 in regulating osteogenic and adipocytic differentiation of hBMSCs, imCL1 cells were transfected with either miR-Control or hsa-miR-4739 and subsequently exposed to osteogenic and adipogenic induction medium. Hsa-miR-4739-trasfected imCL1 exhibited a suppression of differentiation into osteoblastic cells, as evidenced by reduced Alizarin Red S staining for mineralized matrix formation, and confirmed by the quantification of mineralized nodules as well as by the down-regulation of the expression of osteogenic markers (Fig. 5A–C). Moreover, cells overexpressing hsa-miR-4739 exhibited enhanced formation of lipid-filled mature adipocytes (Fig. 5D). Concordant with these data, a higher number of cells were positive for Nile Red staining in imCL1 cultures transfected with hsa-miR-4739 compared to control cultures (Fig. 5E). These findings were confirmed by an adipocyte-specific gene expression assay that revealed over-representation of *aP2* and *PPARg2* (Fig. 5F). These effects of hsa-miR-4739 on hBMSC differentiation were further confirmed by using primary human BMSCs, which provided similar results
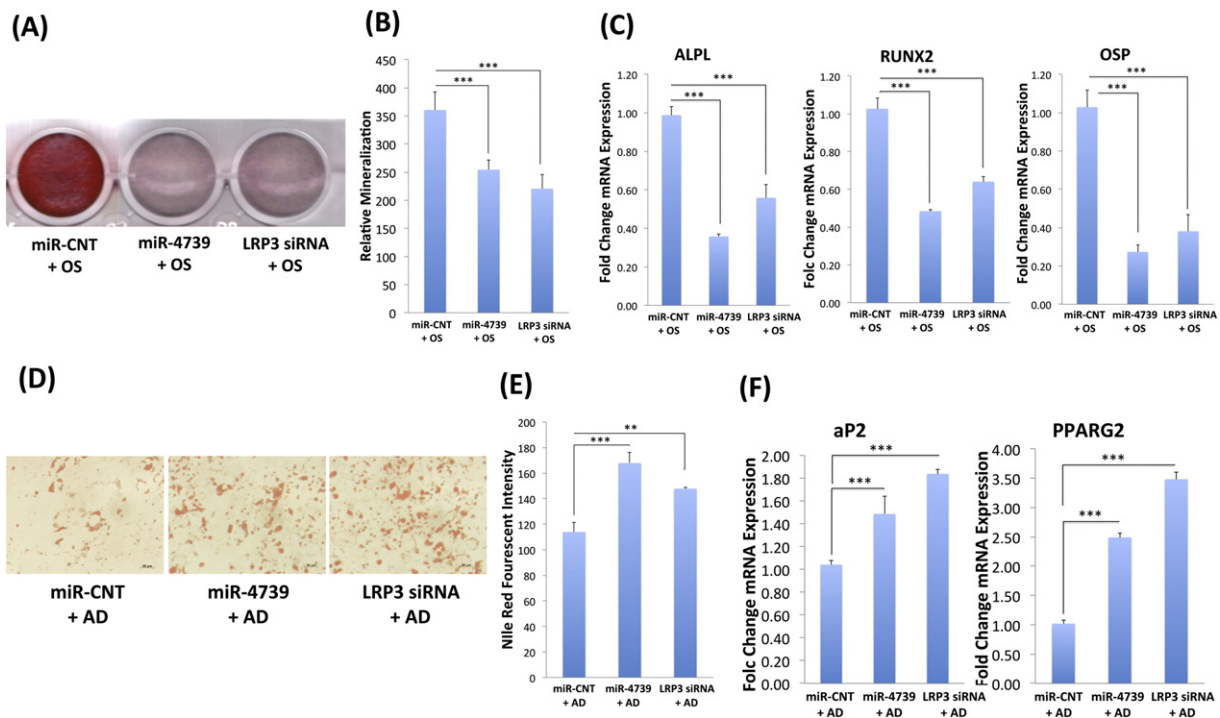


**Fig. 5.** Over-expression of hsa-miR-4793 suppressed osteogenic differentiation and enhanced adipogenic differentiation of imCL1 cells. imCL1 cells were transfected with miR-CNT, miR-4739, or LRP3-siRNA (as a positive control) and then subjected to osteoblastic or adipogenic differentiation induction for 7 days. (A) Mineralized calcium deposition was determined using Alizarin Red S staining for the different treatment groups. (B) Quantification of mineralized nodules using the OsteoImage Mineralization Assay under different transfection conditions. (C) QRT-PCR for osteogenic marker genes (*ALPL*, *RUNX2*, and *OSP*) in miR-CNT-, miR-4739-, or LRP3-siRNA-transfected cells. (D) Oil Red-O staining of accumulated oil droplets in induced imCL1 cells under different treatment conditions. (E) Nile Red staining quantification of oil content in miR-CNT-, miR-4739-, or LRP3-siRNA-transfected imCL1 cells after seven days of adipogenic induction. (F) QRT-PCR quantification of adipogenic markers (*AP2* and *PPARG*) under different treatment conditions. Data are presented as mean ± SD, n = 3. Data are representative of at least two independent experiments; *P < 0.05; **P < 0.01, ***P < 0.005.

(Supplementary Fig. 1). These results suggest a role for hsa-miR-4739-mediated LRP3 suppression in regulating both the osteoblastic and the adipocytic differentiation of hBMSCs. In Fig. 6, we present a schematic model illustrating the novel biological role for miR-4739 as an important regulator of LRP3 activity, promoting inhibition of osteogenic differentiation and enhancement of adipogenic differentiation of hBMSCs through the regulation of several genes and pathways related to osteogenic and adipogenic differentiation.

## 4. Discussion

Identifying regulatory circuits that determine the reciprocal relationship between osteogenic and adipogenic differentiation is necessary for defining the fate of hSSCs/BMSCs and their clinical use in regenerative medicine. In the current study, we established a novel role of LRP3 in regulating the osteogenic and adipogenic differentiation of hBMSCs. Moreover, our data identified hsa-miR-4739 as a molecular switch regulating the balance between osteoblastic and adipocytic differentiation of hBMSCs through the control of LRP3 expression.

It has been reported that the interactions of members of the LRP family trigger a wide range of biological functions, such as endocytosis,

signal transduction, cellular communication, cholesterol control, and vitamin homeostasis (Gotthardt et al., 2000; Li et al., 2001b, 2001a; Nykjaer and Willnow, 2002). LRP5 has been implicated in the regulation of bone mineral density as well as in different types of bone-related diseases through modulation of the Wnt signaling pathway (Haÿ et al., 2009; Xu et al., 2014; Abdallah et al., 2015; Wolski et al., 2015). However, the biological function of LRP3, which exhibits 9.98% homology with LRP5 (as calculated by NCBI protein BLAST) had not yet been described, although LRP3's highest expression is found in skeletal muscles (Ishii et al., 1998). In the current study, we employed a loss-of-function approach to demonstrate the ability of LRP to exert opposing effects on hBMSC osteogenic (enhancement) and adipogenic (inhibition) differentiation, without affecting cell proliferation. It is thus plausible that LRP3 exerts its effects on hBMSCs by enhancing the osteogenic differentiation or by shifting SSC commitment to the osteogenic lineage at the expense of adipogenesis. This hypothesis is supported by microarray-based gene expression data that revealed a number of dysregulated osteogenesis- and adipogenesis-related pathways in LRP3-depleted imCL1 cells, such as regulation of actin cytoskeleton, TGFβ signaling, adipogenesis, endochondral ossification, focal adhesion, and MAPK signaling pathways.
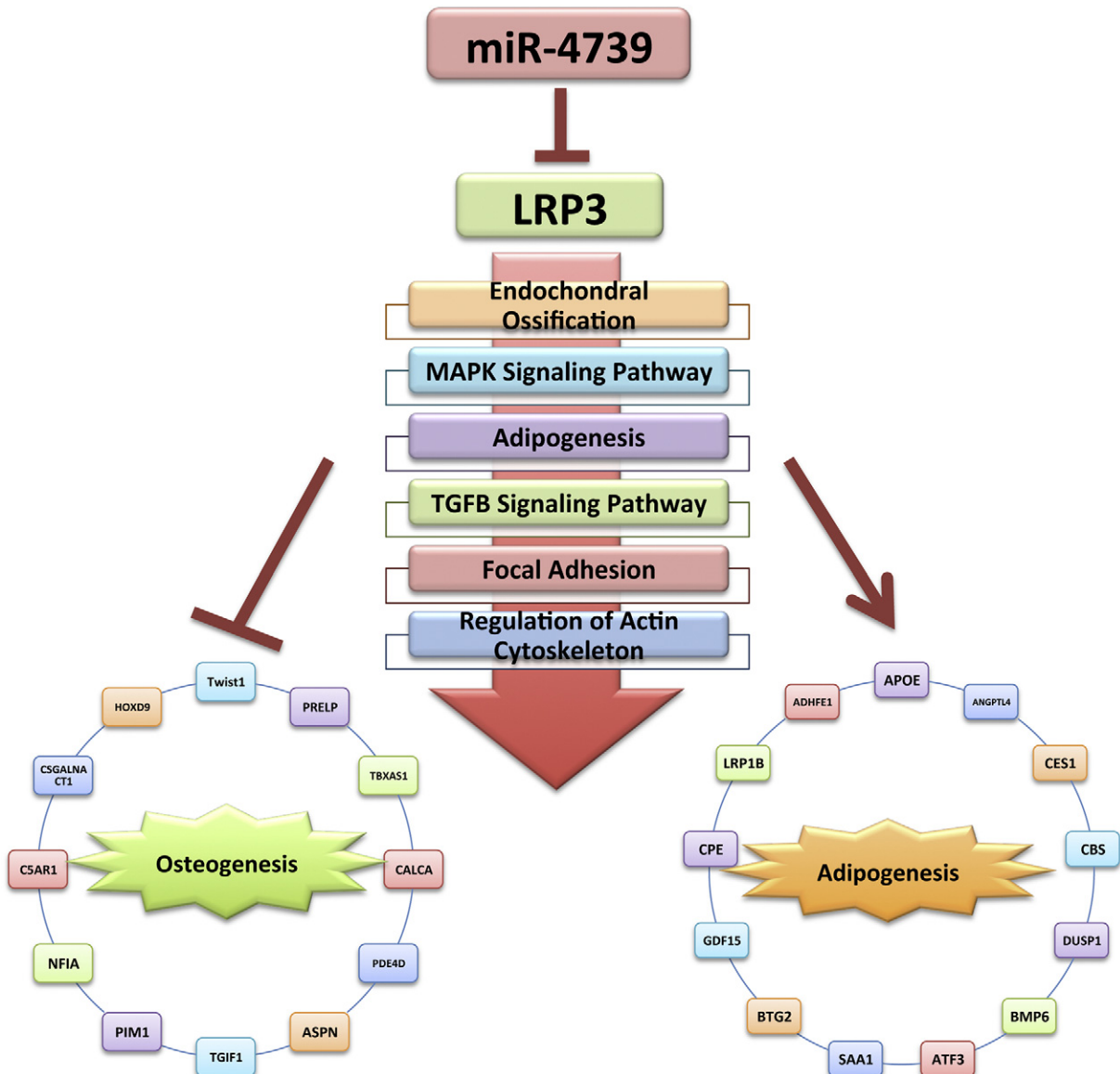


Fig. 6. A proposed schematic model for the novel biological role of miR-4739 as an regulator of LRP3 gene. LRP3 gene inhibition lead to reduced osteogenic and enhancing adipogenic differentiation of hBMSCs through the modulation of several genes and pathways related to osteogenic and adipogenic differentiation.

Several studies have reported pivotal roles for some miRNAs in hBMSC-lineage commitment and fate determination that are mediated by their ability to modulate differentiation-regulating factors. For instance, miR-210, miR-206, miR-133, miR-2861, and miR-138 have been implicated in the regulation of osteogenic differentiation via modulation of the TGFB type I receptor, connexin 43, RUNX2, HDACs, and the FAK, while miR-21, miR-375, miR-27a, and miR-320c have been involved in the regulation of adipogenic differentiation through modulation of TGFB1, ERK1/2, PPARG, and RUNX2 (Eskildsen et al., 2011; Hamam et al., 2014; Hu et al., 2011; Inose et al., 2009; Kim et al., 2010b, 2009; Li et al., 2008; Ling et al., 2011; Mizuno et al., 2009). To identify the molecular mechanism regulating LRP3 expression in hBMSCs, we performed miRNA expression profiling in the imCL1 and imCL2 clones, which revealed some differentially expressed miRNAs between the two clones. Interestingly, hsa-miR-4739, which we subsequently identified as a bone fide regulator of LRP3 expression, was the most under-represented miRNA in imCL1 compared to imCL2. Thus far, only three studies have reported on hsa-miR-4739 functions, linking it to unilineage hematopoietic stem cell differentiation and acute myeloid leukemia, β-catenin signaling pathway and gastric cancer, as well as in the pathogenesis of negative anaplastic large cell lymphoma (Cattaneo et al., 2015; Dong et al., 2015; Wang et al., 2015a). Hence, our data extend the list of possible biological roles of hsa-miR-4739 by demonstrating its ability to regulate LRP3-mediated osteogenic at the expense of adipogenic differentiation of hBMSCs, which suggests that it functions as a molecular switch during hSSC differentiation. It is plausible that hsa-miR-4739 has additional gene targets besides LRP3 that might also regulate hSSC/BMSC osteogenic and adipocytic differentiation. In fact, investigation of the TargetScan database identified LRP4 as a potential target for hsa-miR-4739; however, the direct regulation of LRP4 by hsa-miR-4739 remains to be proven. Therefore, we propose the use of hsa-miR-4739 mimics or inhibitors to fine-tune the commitment of hBMSCs to the osteogenic or the adipogenic lineage, with potential application in regenerative medicine.

Supplementary data to this article can be found online at http://dx.doi.org/10.1016/j.scr.2017.03.001.

## Conflict of interest

The authors declare no conflict of interest.

## Acknowledgements

## References

Abdallah, B.M., Haack-Sørensen, M., Burns, J.S., Elsnab, B., Jakob, F., Hokland, P., Kassem, M., 2005. Maintenance of differentiation potential of human bone marrow mesenchymal stem cells immortalized by human telomerase reverse transcriptase gene despite extensive proliferation. Biochem. Biophys. Res. Commun. 326 (3):527–538. http://dx.doi.org/10.1016/j.bbrc.2004.11.059.

Abdallah, B.M., Jafari, A., Zaher, W., Qiu, W., Kassem, M., 2015. Skeletal (stromal) stem cells: an update on intracellular signaling pathways controlling osteoblast differentiation. Bone 70:28–36. http://dx.doi.org/10.1016/j.bone.2014.07.028.

Alajez, N.M., Lenarduzzi, M., Ito, E., Hui, A.B.Y., Shi, W., Bruce, J., Yue, S., Huang, S.H., Xu, W., Waldron, J., O'Sullivan, B., Liu, F.F., 2011. MiR-218 suppresses nasopharyngeal cancer progression through downregulation of survivin and the SLIT2-ROBO1 pathway. Cancer Res. 71 (6):2381–2391. http://dx.doi.org/10.1158/0008-5472.CAN-10-2754.

Al-Nbaheen, M., Vishnubalaji, R., Ali, D., Bouslimi, A., Al-Jassir, F., Megges, M., Prigione, A., Adjaye, J., Kassem, M., Aldahmash, A., 2013. Human stromal (mesenchymal) stem cells from bone marrow, adipose tissue and skin exhibit differences in molecular phenotype and differentiation potential. Stem Cell Rev. 9 (1):32–43. http://dx.doi.org/10.1007/s12015-012-9365-8.

Ambros, V., 2004. The functions of animal microRNAs. Nature 431 (7006):350–355. http://dx.doi.org/10.1038/nature02871.

Bartel, D.P., 2004. MicroRNAs: genomics, biogenesis, mechanism, and function. Cell 116 (2):281–297. http://dx.doi.org/10.1016/S0092-8674(04)00045-5.

Beresford, J.N., Bennett, J.H., Devlin, C., Leboy, P.S., Owen, M.E., 1992. Evidence for an inverse relationship between the differentiation of adipocytic and osteogenic cells in rat marrow stromal cell cultures. J. Cell Sci. 102 (Pt 2), 341–351.

Bianco, P., Robey, P.G., 2004. Skeletal stem cells. In: Lanza, R.P. (Ed.), Handbook of Adult and Fetal Stem Cells. Academic Press, San Diego, pp. 415–424.

Caplan, A.I., 1991. Mesenchymal stem cells. J. Orthop. Res. 9:641–650. http://dx.doi.org/10.1002/jor.1100090504.

Cattaneo, M., Pelosi, E., Castelli, G., Cerio, A.m., D'angiò, A., Porretti, L., Rebulla, P., Pavesi, L., Russo, G., Giordano, A., Turri, J., Cicconi, L., Lo-Coco, F., Testa, U., Biunno, I., 2015. A miRNA signature in human cord blood stem and progenitor cells as potential biomarker of specific acute myeloid leukemia subtypes. J. Cell. Physiol. 230: 1770–1780. http://dx.doi.org/10.1002/jcp.24876.

Chen, L., Jiang, C., Tiwari, S.R., Shrestha, A., Xu, P., Liang, W., Sun, Y., He, S., Cheng, B., 2015. TGIF1 gene silencing in tendon-derived stem cells improves the tendon-to-bone insertion site regeneration. Cell. Physiol. Biochem. 37 (6):2101–2114. http://dx.doi.org/10.1159/000438568.

Chiba, T., Nakazawa, T., Yui, K., Kaneko, E., Shimokado, K., 2003. VLDL induces adipocyte differentiation in ApoE-dependent manner. Arterioscler. Thromb. Vasc. Biol. 23 (8): 1423–1429. http://dx.doi.org/10.1161/01.ATV.0000085040.58340.36.

Clément-Lacroix, P., Ai, M., Morvan, F., Roman-Roman, S., Vayssière, B., Belleville, C., Estrera, K., Warman, M.L., Baron, R., Rawadi, G., 2005. Lrp5-independent activation of Wnt signaling by lithium chloride increases bone formation and bone mass in mice. Proc. Natl. Acad. Sci. U. S. A. 102 (48):17406–17411. http://dx.doi.org/10.1073/pnas.0505259102.

Croy, J.E., Shin, W.D., Knauer, M.F., Knauer, D.J., Komives, E.A., 2003. All three LDL receptor homology regions of the LDL receptor-related protein bind multiple ligands. Biochemistry 42 (44):13049–13057. http://dx.doi.org/10.1021/bi034752s.

Dong, S., Yang, B., Guo, H., Kang, F., 2012. MicroRNAs regulate osteogenesis and chondrogenesis. Biochem. Biophys. Res. Commun. 418 (4):587–591. http://dx.doi.org/10.1016/j.bbrc.2012.01.075.

Dong, L., Deng, J., Sun, Z.-M., Pan, A.-P., Xiang, X.-J., Zhang, L., Yu, F., Chen, J., Sun, Z., Feng, M., Xiong, J.P., 2015. Interference with the β-catenin gene in gastric cancer induces changes to the miRNA expression profile. Tumour Biol. 36 (9):6973–6983. http://dx.doi.org/10.1007/s13277-015-3415-1.

Driller, K., Pagenstecher, A., Uhl, M., Omran, H., Berlis, A., Gründer, A., Sippel, A.E., 2007. Nuclear factor I X deficiency causes brain malformation and severe skeletal defects. Mol. Cell. Biol. 27 (10):3855–3867. http://dx.doi.org/10.1128/MCB.02293-06.

Elsafadi, M., Manikandan, M., Atteya, M., Hashmi, J.A., Iqbal, Z., Aldahmash, A., Alfayez, M., Kassem, M., Mahmood, A., 2016. Characterization of cellular and molecular heterogeneity of bone marrow stromal cells. Stem Cells Int. 2016:9378081. http://dx.doi.org/10.1155/2016/9378081.

Eskildsen, T., Taipaleenmäki, H., Stenvang, J., Abdallah, B.M., Ditzel, N., Nossent, A.Y., Bak, M., Kauppinen, S., Kassem, M., 2011. MicroRNA-138 regulates osteogenic differentiation of human stromal (mesenchymal) stem cells in vivo. Proc. Natl. Acad. Sci. U. S. A. 108 (15):6139–6144. http://dx.doi.org/10.1073/pnas.1016758108.

Ferguson, B.S., Nam, H., Stephens, J.M., Morrison, R.F., 2015. Mitogen-dependent regulation of DUSP1 governs ERK and p38 signaling during early 3T3-L1 adipocyte differentiation. J. Cell. Physiol. 231 (7):1562–1574. http://dx.doi.org/10.1002/jcp.25248.

Friedenstein, A.Y., 1968. Induction of bone tissue by transitional epithelium. Clin. Orthop. 59, 21–37.

Friedenstein, A.J., 1976. Precursor cells of mechanocytes. Int. Rev. Cytol. 47, 327–359.

Friedenstein, A.J., Piatetzky-Shapiro, I.I., Petrakova, K.V., 1966. Osteogenesis in transplants of bone marrow cells. J. Embryol. Exp. Morpholog. 16 (3), 381–390.

Fromental-Ramain, C., Warot, X., Lakkaraju, S., Favier, B., Haack, H., Birling, C., Dierich, A., Doll e, P., Chambon, P., 1996. Specific and redundant functions of the paralogous Hoxa-9 and Hoxd-9 genes in forelimb and axial skeleton patterning. Dev. Camb. Engl. 122, 461–472.

Garcia, C.K., Wilund, K., Arca, M., Zuliani, G., Fellin, R., Maioli, M., Calandra, S., Bertolini, S., Cossu, F., Grishin, N., Barnes, R., Cohen, J.C., Hobbs, H.H., 2001. Autosomal recessive hypercholesterolemia caused by mutations in a putative LDL receptor adaptor protein. Science 292 (5520):1394–1398. http://dx.doi.org/10.1126/science.1060458.

Geneviève, D., Proulle, V., Isidor, B., Bellais, S., Serre, V., Djouadi, F., Picard, C., Vignon-Savoye, C., Bader-Meunier, B., Blanche, S., de Vernejoul, M.C., Legeai-Mallet, L., Fischer, A.M., Le Merrer, M., Dreyfus, M., Gaussem, P., Munnich, A., Cormier-Daire, V., 2008. Thromboxane synthase mutations in an increased bone density disorder (Ghosal syndrome). Nat. Genet. 40 (3):284–286. http://dx.doi.org/10.1038/ng.2007.66.

Gimble, J.M., Nuttall, M.E., 2004. Bone and fat: old questions, new insights. Endocrine 23 (2–3):183–188. http://dx.doi.org/10.1385/ENDO:23:2-3:183.

Gimble, J.M., Robinson, C.E., Wu, X., Kelly, K.A., 1996. The function of adipocytes in the bone marrow stroma: an update. Bone 19 (5):421–428. http://dx.doi.org/10.1016/S8756-3282(96)00258-X.

Goretzki, L., Mueller, B.M., 1998. Low-density-lipoprotein-receptor-related protein (LRP) interacts with a GTP-binding protein. Biochem. J. 336 (2):381–386. http://dx.doi.org/10.1042/bj3360381.

Gotthardt, M., Trommsdorff, M., Nevitt, M.F., Shelton, J., Richardson, J.A., Stockinger, W., Nimpf, J., Herz, J., 2000. Interactions of the low density lipoprotein receptor gene family with cytosolic adaptor and scaffold proteins suggest diverse biological functions in cellular communication and signal transduction. J. Biol. Chem. 275 (33): 25616–25624. http://dx.doi.org/10.1074/jbc.M000955200.

Gregory, C.A., Gunn, W.G., Peister, A., Prockop, D.J., 2004. An Alizarin red-based assay of mineralization by adherent cells in culture: comparison with cetylpyridinium chloride extraction. Anal. Biochem. 329 (1):77–84. http://dx.doi.org/10.1016/j.ab.2004.02.002.

Hamam, D., Ali, D., Vishnubalaji, R., Hamam, R., Al-Nbaheen, M., Chen, L., Kassem, M., Aldahmash, A., Alajez, N.M., 2014. microRNA-320/RUNX2 axis regulates adipocytic

differentiation of human mesenchymal (skeletal) stem cells. Cell Death Dis. 5:e1499. http://dx.doi.org/10.1038/cddis.2014.462.

Haÿ, E., Laplantine, E., Geoffroy, V., Frain, M., Kohler, T., Müller, R., Marie, P.J., 2009. N-cadherin interacts with axin and LRP5 to negatively regulate Wnt/beta-catenin signaling, osteoblast function, and bone formation. Mol. Cell. Biol. 29 (4):953–964. http://dx.doi.org/10.1128/MCB.00349-08.

Hildebrand, A., Romarís, M., Rasmussen, L.M., Heinegård, D., Twardzik, D.R., Border, W.A., Ruoslahti, E., 1994. Interaction of the small interstitial proteoglycans biglycan, decorin and fibromodulin with transforming growth factor beta. Biochem. J. 302 (2): 527–534. http://dx.doi.org/10.1042/bj3020527.

Hu, R., Liu, W., Li, H., Yang, L., Chen, C., Xia, Z.-Y., Guo, L.-J., Xie, H., Zhou, H.-D., Wu, X.P., Luo, X.H., 2011. A Runx2/miR-3960/miR-2861 regulatory feedback loop during mouse osteoblast differentiation. J. Biol. Chem. 286 (14):12328–12339. http://dx.doi.org/10.1074/jbc.M110.176099.

Huang, Y., Shen, X.J., Zou, Q., Wang, S.P., Tang, S.M., Zhang, G.Z., 2010. Biological functions of microRNAs: a review. J. Physiol. Biochem. 67 (1):129–139. http://dx.doi.org/10.1007/s13105-010-0050-6.

Huebner, A.K., Keller, J., Catala-Lehnen, P., Perkovic, S., Streichert, T., Emeson, R.B., Amling, M., Schinke, T., 2008. The role of calcitonin and alpha-calcitonin gene-related peptide in bone formation. Arch. Biochem. Biophys. 473 (2):210–217. http://dx.doi.org/10.1016/j.abb.2008.02.013.

Inose, H., Ochi, H., Kimura, A., Fujita, K., Xu, R., Sato, S., Iwasaki, M., Sunamura, S., Takeuchi, Y., Fukumoto, S., Saito, K., Nakamura, T., Siomi, H., Ito, H., Arai, Y., Shinomiya, K., Takeda, S., 2009. A microRNA regulatory mechanism of osteoblast differentiation. Proc. Natl. Acad. Sci. 106 (49):20794–20799. http://dx.doi.org/10.1073/pnas.0909311106.

Ishii, H., Kim, D.H., Fujita, T., Endo, Y., Saeki, S., Yamamoto, T.T., 1998. cDNA cloning of a new low-density lipoprotein receptor-related protein and mapping of its gene (LRP3) to chromosome bands 19q12–q13.2. Genomics 51 (1):132–135. http://dx.doi.org/10.1006/geno.1998.5339.

Jang, M.K., Jung, M.H., 2014. ATF3 represses PPARγ expression and inhibits adipocyte differentiation. Biochem. Biophys. Res. Commun. 454 (1):58–64. http://dx.doi.org/10.1016/j.bbrc.2014.10.028.

Jeong, Y.H., Ishikawa, K., Someya, Y., Hosoda, A., Yoshimi, T., Yokoyama, C., Kiryu-Seo, S., Kang, M.J., Tchibana, T., Kiyama, H., Fukumura, T., Kim, D.H., Saeki, S., 2010. Molecular characterization and expression of the low-density lipoprotein receptor-related protein-10, a new member of the LDLR gene family. Biochem. Biophys. Res. Commun. 391 (1):1110–1115. http://dx.doi.org/10.1016/j.bbrc.2009.12.033.

Jernås, M., Olsson, B., Arner, P., Jacobson, P., Sjöström, L., Walley, A., Froguel, P., McTernan, P.G., Hoffstedt, J., Carlsson, L.M.S., 2009. Regulation of carboxylesterase 1 (CES1) in human adipose tissue. Biochem. Biophys. Res. Commun. 383 (1):63–67. http://dx.doi.org/10.1016/j.bbrc.2009.03.120.

Jia, S., Zhai, H., Zhao, M., 2014. MicroRNAs regulate immune system via multiple targets. Discov. Med. 18 (100), 237–247.

Kalbasi Anaraki, P., Patecki, M., Larmann, J., Tkachuk, S., Jurk, K., Haller, H., Theilmeier, G., Dumler, I., 2014. Urokinase receptor mediates osteogenic differentiation of mesenchymal stem cells and vascular calcification via the complement C5a receptor. Stem Cells Dev. 23 (4):352–362. http://dx.doi.org/10.1089/scd.2013.0318.

Kato, M., Patel, M.S., Levasseur, R., Lobov, I., Chang, B.H., Glass 2nd, D.A., Hartmann, C., Li, L., Hwang, T.H., Brayton, C.F., Lang, R.A., Karsenty, G., Chan, L., 2002. Cbfa1-independent decrease in osteoblast proliferation, osteopenia, and persistent embryonic eye vascularization in mice deficient in Lrp5, a Wnt coreceptor. J. Cell Biol. 157 (2): 303–314. http://dx.doi.org/10.1083/jcb.200201089.

Kim, J.Y., Tillison, K.S., Zhou, S., Lee, J.H., Smas, C.M., 2007. Differentiation-dependent expression of Adhfe1 in adipogenesis. Arch. Biochem. Biophys. 464 (1):100–111. http://dx.doi.org/10.1016/j.abb.2007.04.018.

Kim, Y.J., Hwang, S.J., Bae, Y.C., Jung, J.S., 2009. MiR-21 regulates adipogenic differentiation through the modulation of TGF-beta signaling in mesenchymal stem cells derived from human adipose tissue. Stem Cells 27 (12):3093–3102. http://dx.doi.org/10.1002/stem.235.

Kim, S.Y., Kim, A.Y., Lee, H.W., Son, Y.H., Lee, G.Y., Lee, J.-W., Lee, Y.S., Kim, J.B., 2010a. miR-27a is a negative regulator of adipocyte differentiation via suppressing PPARgamma expression. Biochem. Biophys. Res. Commun. 392 (3):323–328. http://dx.doi.org/10.1016/j.bbrc.2010.01.012.

Kim, K., Kim, J.H., Youn, B.U., Jin, H.M., Kim, N., 2010b. Pim-1 regulates RANKL-induced osteoclastogenesis via NF-κB activation and NFATc1 induction. J. Immunol. 185 (12): 7460–7466 Baltim. Md 1950. 10.4049/jimmunol.1000885.

Kim, S., Hong, J.-W., Park, K.W., 2016. B cell translocation gene 2 (Btg2) is regulated by Stat3 signaling and inhibits adipocyte differentiation. Mol. Cell. Biochem. 413 (1–2):145–153. http://dx.doi.org/10.1007/s11010-015-2648-z.

Kozomara, A., Griffiths-Jones, S., 2011. miRBase: integrating microRNA annotation and deep-sequencing data. Nucleic Acids Res. 39:D152–D157. http://dx.doi.org/10.1093/nar/gkq1027.

Laine, S.K., Hentunen, T., Laitala-Leinonen, T., 2012a. Do microRNAs regulate bone marrow stem cell niche physiology? Gene 497 (1):1–9. http://dx.doi.org/10.1016/j.gene.2012.01.045.

Laine, S.K., Alm, J.J., Virtanen, S.P., Aro, H.T., Laitala-Leinonen, T.K., 2012b. MicroRNAs miR-96, miR-124, and miR-199a regulate gene expression in human bone marrow-derived mesenchymal stem cells. J. Cell. Biochem. 113 (8):2687–2695. http://dx.doi.org/10.1002/jcb.24144.

Li, Y., Lu, W., Marzolo, M.P., Bu, G., 2001a. Differential functions of members of the low density lipoprotein receptor family suggested by their distinct endocytosis rates. J. Biol. Chem. 276 (21):18000–18006. http://dx.doi.org/10.1074/jbc.M101589200.

Li, Y., Cam, J., Bu, G., 2001b. Low-density lipoprotein receptor family. Mol. Neurobiol. 23 (1):53–67. http://dx.doi.org/10.1385/MN:23:1:53.

Li, Z., Hassan, M.Q., Volinia, S., van Wijnen, A.J., Stein, J.L., Croce, C.M., Lian, J.B., Stein, G.S., 2008. A microRNA signature for a BMP2-induced osteoblast lineage commitment

program. Proc. Natl. Acad. Sci. 105 (37):13906–13911. http://dx.doi.org/10.1073/pnas.0804438105.

Ling, H.Y., Wen, G.B., Feng, S.D., Tuo, Q.H., Ou, H.S., Yao, C.H., Zhu, B.Y., Gao, Z.P., Zhang, L., Liao, D.F., 2011. MicroRNA-375 promotes 3T3-L1 adipocyte differentiation through modulation of extracellular signal-regulated kinase signalling. Clin. Exp. Pharmacol. Physiol. 38 (4):239–246. http://dx.doi.org/10.1111/j.1440-1681.2011.05493.x.

Masson, O., Chavey, C., Dray, C., Meulle, A., Daviaud, D., Quilliot, D., Muller, C., Valet, P., Liaudet-Coopman, E., 2009. LRP1 receptor controls adipogenesis and is up-regulated in human and mouse obese adipose tissue. PLoS One 4 (10):e7422. http://dx.doi.org/10.1371/journal.pone.0007422.

Min, S.Y., Yang, H., Seo, S.G., Shin, S.H., Chung, M.Y., Kim, J., Lee, S.J., Lee, H.J., Lee, K.W., 2005. 2013. Cocoa polyphenols suppress adipogenesis in vitro and obesity in vivo by targeting insulin receptor. Int. J. Obes. 37 (4):584–592. http://dx.doi.org/10.1038/ijo.2012.85.

Mizuno, Y., Tokuzawa, Y., Ninomiya, Y., Yagi, K., Yatsuka-Kanesaki, Y., Suda, T., Fukuda, T., Katagiri, T., Kondoh, Y., Amemiya, T., Tashiro, H., Okazaki, Y., 2009. miR-210 promotes osteoblastic differentiation through inhibition of AcvR1b. FEBS Lett. 583 (13): 2263–2268. http://dx.doi.org/10.1016/j.febslet.2009.06.006.

Nykjaer, A., Willnow, T.E., 2002. The low-density lipoprotein receptor gene family: a cellular Swiss army knife? Trends Cell Biol. 12 (6):273–280. http://dx.doi.org/10.1016/S0962-8924(02)02282-1.

Owen, M., Friedenstein, A.J., 1988. Stromal stem cells: marrow-derived osteogenic precursors. CIBA Found. Symp. 136, 42–60.

Papaioannou, G., Mirzamohammadi, F., Kobayashi, T., 2014. MicroRNAs involved in bone formation. Cell. Mol. Life Sci. 71 (24):4747–4761. http://dx.doi.org/10.1007/s00018-014-1700-6.

Pi, C., Li, Y.P., Zhou, X., Gao, B., 2015. The expression and function of microRNAs in bone homeostasis. Front. Biosci. (Landmark Ed.) 20:119–138. http://dx.doi.org/10.2741/4301.

Pillai, R.S., 2005. MicroRNA function: multiple mechanisms for a tiny RNA? RNA 11 (2): 1753–1761. http://dx.doi.org/10.1261/rna.2248605.

Quarto, N., Senarath-Yapa, K., Renda, A., Longaker, M.T., 2015. TWIST1 silencing enhances in vitro and in vivo osteogenic differentiation of human adipose-derived stem cells by triggering activation of BMP-ERK/FGF signaling and TAZ upregulation. Stem Cells 33 (3):833–847. http://dx.doi.org/10.1002/stem.1907.

Sato, T., Kudo, T., Ikehara, Y., Ogawa, H., Hirano, T., Kiyohara, K., Hagiwara, K., Togayachi, A., Ema, M., Takahashi, S., Kimata, K., Watanabe, H., Narimatsu, H., 2011. Chondroitin sulfate N-acetylgalactosaminyltransferase 1 is necessary for normal endochondral ossification and aggrecan metabolism. J. Biol. Chem. 286 (7):5803–5812. http://dx.doi.org/10.1074/jbc.M110.159244.

Serra, R., Chang, C., 2003. TGF-beta signaling in human skeletal and patterning disorders. Birth Defects Res. C Embryo Today 69 (4):333–351. http://dx.doi.org/10.1002/bdrc.10023.

Sharma, A., Huard, C., Vernochet, C., Ziemek, D., Knowlton, K.M., Tyminski, E., Paradis, T., Zhang, Y., Jones, J.E.C., von Schack, D., Brown, C.T., Milos, P.M., Coyle, A.J., Tremblay, F., Martinez, R.V., 2014. Brown fat determination and development from muscle precursor cells by novel action of bone morphogenetic protein 6. PLoS One 9 (3):e92608. http://dx.doi.org/10.1371/journal.pone.0092608.

Skårn, M., Namløs, H.M., Noordhuis, P., Wang, M.Y., Meza-Zepeda, L.A., Myklebost, O., 2012. Adipocyte differentiation of human bone marrow-derived stromal cells is modulated by microRNA-155, microRNA-221, and microRNA-222. Stem Cells Dev. 21 (6): 873–883. http://dx.doi.org/10.1089/scd.2010.0503.

Strickland, D.K., Kounnas, M.Z., Williams, S.E., Argraves, W.S., 1994. LDL receptor-related protein (LRP): a multiligand receptor. Fibrinolysis 8. Supplement 1:204–215. http://dx.doi.org/10.1016/0268-9499(94)90718-8.

Tétreault, N., De Guire, V., 2013. miRNAs: their discovery, biogenesis and mechanism of action. Clin. Biochemist 46 (10−11):842–845. http://dx.doi.org/10.1016/j.clinbiochem.2013.02.009.

Trommsdorff, M., Gotthardt, M., Hiesberger, T., Shelton, J., Stockinger, W., Nimpf, J., Hammer, R.E., Richardson, J.A., Herz, J., 1999. Reeler/disabled-like disruption of neuronal migration in knockout mice lacking the VLDL receptor and ApoE receptor 2. Cell 97 (6):689–701. http://dx.doi.org/10.1016/S0092-8674(00)80782-5.

Tsai, C.Y., Peh, M.T., Feng, W., Dymock, B.W., Moore, P.K., 2015. Hydrogen sulfide promotes adipogenesis in 3T3L1 cells. PLoS One 10 (3):e0119511. http://dx.doi.org/10.1371/journal.pone.0119511.

Ueda, M., Goto, T., Kuroishi, K.N., Gunjigake, K.K., Ikeda, E., Kataoka, S., Nakatomi, M., Toyono, T., Seta, Y., Kawamoto, T., 2016. Asporin in compressed periodontal ligament cells inhibits bone formation. Arch. Oral Biol. 62:86–92. http://dx.doi.org/10.1016/j.archoralbio.2015.11.010.

Vishnubalaji, R., Hamam, R., Yue, S., Al-Obeed, O., Kassem, M., Liu, F.F., Aldahmash, A., Alajez, N.M., 2016. MicroRNA-320 suppresses colorectal cancer by targeting SOX4, FOXM1, and FOXQ1. Oncotarget 7 (24):35789–35802. http://dx.doi.org/10.18632/oncotarget.8937.

Wakabayashi, S., Tsutsumimoto, T., Kawasaki, S., Kinoshita, T., Horiuchi, H., Takaoka, K., 2002. Involvement of phosphodiesterase isozymes in osteoblastic differentiation. J. Bone Miner. Res. 17 (2):249–256. http://dx.doi.org/10.1359/jbmr.2002.17.2.249.

Wang, Y.C., Kuo, W.H., Chen, C.Y., Lin, H.Y., Wu, H.T., Liu, B.H., Chen, C.H., Mersmann, H.J., Chang, K.J., Ding, S.T., 2010. Docosahexaenoic acid regulates serum amyloid A protein to promote lipolysis through down regulation of perilipin. J. Nutr. Biochem. 21 (4): 317–324. http://dx.doi.org/10.1016/j.jnutbio.2009.01.004.

Wang, C., Chen, X., Chen, X., He, Y., Cao, L., 2015a. Expression of microRNA in ALK-negative anaplastic large cell lymphoma and CD30-positive peripheral T cell lymphoma, not otherwise specified. Zhonghua Bing Li Xue Za Zhi 44 (8), 565–570.

Wang, C.Y., Shie, S.S., Wen, M.S., Hung, K.C., Hsieh, I.C., Yeh, T.S., Wu, D., 2015b. Loss of FTO in adipose tissue decreases Angptl4 translation and alters triglyceride metabolism. Sci. Signal. 8 (407):ra127. http://dx.doi.org/10.1126/scisignal.aab3357.

Williams, B.O., Insogna, K.L., 2009. Where Wnts went: the exploding field of Lrp5 and Lrp6 signaling in bone. J. Bone Miner. Res. 24 (2):171–178. http://dx.doi.org/10.1359/jbmr.081235.

Wolski, H., Drwęska-Matelska, N., Seremak-Mrozikiewicz, A., Łowicki, Z., Czerny, B., 2015. The role of Wnt/β-catenin pathway and LRP5 protein in metabolism of bone tissue and osteoporosis etiology. Ginekol. Pol. 86 (4), 311–314.

Xu, G.Y., Qiu, Y., Mao, H.J., 2014. Common polymorphism in the LRP5 gene may increase the risk of bone fracture and osteoporosis. Biomed. Res. Int. 2014:290531. http://dx.doi.org/10.1155/2014/290531.

Yanagitai, M., Kitagawa, T., Okawa, K., Koyama, H., Satoh, T., 2012. Phenylenediamine derivatives induce GDF-15/MIC-1 and inhibit adipocyte differentiation of mouse 3T3-L1 cells. Biochem. Biophys. Res. Commun. 417 (1):294–298. http://dx.doi.org/10.1016/j.bbrc.2011.11.103.

Yokota, T., Meka, C.S., Medina, K.L., Igarashi, H., Comp, P.C., Takahashi, M., Nishida, M., Oritani, K., Miyagawa, J.I., Funahashi, T., Tomiyama, Y., Matsuzawa, Y., Kincade, P.W., 2002. Paracrine regulation of fat cell formation in bone marrow cultures via adiponectin and prostaglandins. J. Clin. Invest. 109 (10):1303–1310. http://dx.doi.org/10.1172/JCI14506.

Yokota, T., Meka, C.S., Kouro, T., Medina, K.L., Igarashi, H., Takahashi, M., Oritani, K., Funahashi, T., Tomiyama, Y., Matsuzawa, Y., Kincade, P.W., 2003. Adiponectin, a fat cell product, influences the earliest lymphocyte precursors in bone marrow cultures by activation of the cyclooxygenase-prostaglandin pathway in stromal cells. J. Immunol. 171 (10):5091–5099 BaltimMd 1950. 10.4049/jimmunol.171.10.5091.